

Embed Progressive Implicit Preference in Unified Space for Deep Collaborative Filtering

Zhongjin Zhang*
Central South University
Changsha, China
zhangzhongjin@csu.edu.cn

Yu Liang*
Central South University
Changsha, China
yl8373713@gmail.com

Cong Fu
Shopee Pte. Ltd.
Singapore, Singapore
fc731097343@gmail.com

Yuxuan Zhu
Shopee Pte. Ltd.
Shanghai, China
iamyuxuanzhu@gmail.com

Kun Wang
Shopee Pte. Ltd.
Shanghai, China
wk1135256721@gmail.com

Yabo Ni
Nanyang Technological University
Singapore, Singapore
yabo001@e.ntu.edu.sg

Anxiang Zeng
SCSE, Nanyang Technological
University
Singapore, Singapore
zeng0118@e.ntu.edu.sg

Jiazhi Xia[†]
Central South University
Changsha, China
xiajiazhi@csu.edu.cn

ABSTRACT

Embedding-based collaborative filtering, often coupled with nearest neighbor search, is widely deployed in large-scale recommender systems for personalized content selection. Modern systems leverage multiple implicit feedback signals (e.g., clicks, add to cart, purchases) to model user preferences comprehensively. However, prevailing approaches adopt a feedback-wise modeling paradigm, which (1) fails to capture the structured progression of user engagement entailed among different feedback and (2) embeds feedback-specific information into disjoint spaces, making representations incommensurable, increasing system complexity, and leading to suboptimal retrieval performance. A promising alternative is Ordinal Logistic Regression (OLR), which explicitly models discrete ordered relations. However, existing OLR-based recommendation models mainly focus on explicit feedback (e.g., movie ratings) and struggle with implicit, correlated feedback, where ordering is vague and non-linear. Moreover, standard OLR lacks flexibility in handling feedback-dependent covariates, resulting in suboptimal performance in real-world systems. To address these limitations, we propose Generalized Neural Ordinal Logistic Regression (GNOLR), which encodes multiple feature-feedback dependencies into a unified, structured embedding space and enforces feedback-specific dependency learning through a nested optimization framework. Thus, GNOLR enhances predictive accuracy, captures the progression of user engagement, and simplifies the retrieval process. We establish a theoretical comparison with existing paradigms, demonstrating how GNOLR avoids disjoint spaces while maintaining effectiveness. Extensive experiments on ten real-world datasets show that GNOLR significantly outperforms state-of-the-art methods in efficiency and adaptability.

1 INTRODUCTION

To mitigate information overload, embedding-based collaborative filtering (CF) [19, 45] has become the foundation of large-scale

*Equal contribution.

[†]Corresponding author.

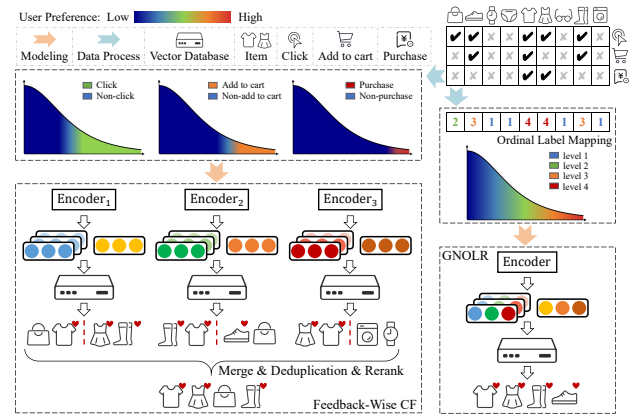


Figure 1: An illustration comparing the prior paradigm with GNOLR. Prior methods embed entities into feedback-wise, incommensurable spaces, requiring separate ranking and fusion before displaying to users. In contrast, GNOLR unifies various feedback in a shared embedding space, aligning the spatial proximity with the user preference progression for seamless one-stage ranking and improved prediction.

recommender systems (RS), enabling personalized item selection and ranking. In practice, CF is often paired with nearest neighbor search (NNS) [8, 12, 26, 35] for efficient retrieval, ensuring that relevant candidates are quickly surfaced for users [7]. Modern RS increasingly rely on multiple implicit feedback signals, e.g., click/like a video or click/purchase a commodity, to infer user preferences [11, 23, 47, 53, 62]. These pieces of feedback reflect different levels of user engagement, making it crucial to model them holistically. However, prevalent embedding-based CF methods face **three fundamental limitations** that hinder their effectiveness:

(1) They treat each feedback type as an independent binary classification or ranking task, overlooking the underlying progression in

user engagement. For instance, in purchase prediction, clicked but unpurchased items are treated as equally negative as non-clicked items. However, semantically, the former is preferred over the latter. This simplification can lead to misinterpretation of user intent.

(2) Task-wise modeling produces disjoint embedding spaces for each feedback type, making them incommensurable: the similarity scores computed in one space cannot be meaningfully compared to those from another. This fragmentation prevents a unified candidate retrieval process (Figure 1). As a result, large-scale RS, which rely on efficient NNS [15], suffer from redundant indexing and ranking. In addition, because scores from different tasks follow different scales and distributions, fusion heuristics such as additive or multiplicative aggregation [40, 41, 60] often introduce accuracy loss and distort user preferences. This not only increases system complexity as the number of tasks grows but also degrades recommendation quality.

(3) Task-wise modeling employs separate prediction heads for different feedback labels. When feedback labels contradict each other (e.g., clicked but unpurchased), gradient conflicts arise in shared parameters, negatively impacting learning stability [20, 56].

Ordinal Logistic Regression (OLR) [37] has been applied in RS [22, 28] to model progressiveness over explicit ratings, offering potential for progressive implicit feedback. However, applying standard OLR in this context also introduces **key challenges**:

(1) Unlike ratings, implicit feedback does not always follow a rigid sequence (e.g., users may follow an influencer without "liking" their videos). This violates OLR's strict ordinal assumption.

(2) Standard OLR [37] applies the same set of regression coefficients to all feedback types, assuming a uniform relationship between features and different levels of user engagement. However, feedback like clicks and purchases are influenced by distinct factors (e.g., click-through rate vs. sales count). Simply introducing separate coefficients or networks for each feedback type may address this limitation, but it **reintroduces disjoint embedding spaces**.

To address these challenges, we propose **Generalized Neural Ordinal Logistic Regression (GNOLR)**, a novel framework that integrates ordinal modeling with neural representation learning for implicit feedback. Our key contributions are as follows:

(1) We introduce an ordinal mapping technique to transform unstructured implicit feedback into strictly ordered labels, enabling effective ordinal modeling. GNOLR employs a nested optimization framework that captures feedback-specific feature dependencies while embedding underlying user preferences in a unified space, enabling a single NNS process without compromising accuracy.

(2) We provide theoretical analysis demonstrating how GNOLR's embedding similarity structure aligns with the progression of user engagement and highlight its advantages over traditional feedback-wise multi-task approaches.

(3) Extensive experiments on ten real-world datasets show that GNOLR achieves state-of-the-art performance, significantly improving both ranking accuracy and retrieval effectiveness.

2 PRELIMINARY

2.1 Notations

We differentiate vectors and scalars in bold font, e.g., a vector \mathbf{x} and a scalar x . A random variable and its realization are differentiated by italic font, for example, the vector-valued random variable \mathbf{x} and its

realization \mathbf{x} . Let \mathcal{U} denote the set of users and \mathcal{I} denote the set of items. Let $Y = \{y_1, y_2, \dots, y_T\}$ represent the label set corresponding to T types of implicit feedback, where each $y_i \in \{0, 1\}$. Let $\mathcal{D} = \{(\mathbf{x}_u, \mathbf{x}_i, Y_{u,i})\}$ denote the observed samples, where $\mathbf{x}_u, \mathbf{x}_i$ are the feature vectors for the users and the items.

2.2 Problem Formulation and Challenges

The ultimate goal of leveraging various implicit feedback signals in RS is to achieve a unified and comprehensive understanding of the preference progression in user interactions. This is often overlooked in current literature. To push the research a step further toward real-world applicability, this paper focuses on a new problem:

2.2.1 Multi-Feedback Collaborative Filtering (MFCF). MFCF aims to jointly model multiple types of implicit feedback (e.g., clicks, add to cart, purchases) to generate a **global ranking of candidate items** for display to users. Formally, for a given user $u \in \mathcal{U}$, the objective is to rank a set of candidate items \mathcal{I} by leveraging all available feedback signals Y to generate a unified global ranking list $\mathcal{L}(u) = [i_1, i_2, \dots, i_m]$, where $i_j \preceq_u i_k$ if $j < k$. Here, \preceq_u denotes that user u prefers item i_j over i_k .

In collaborative filtering, this corresponds to learning embeddings for u and i , and a scoring function \mathcal{K} such that $\mathcal{K}(u, i_j) > \mathcal{K}(u, i_k)$ implies $i_j \preceq_u i_k$. Predominant paradigms utilize neural networks to extract user and item representations [25, 55, 57] and employ kernel functions for similarity measures [24, 25, 59].

2.3 Ordinal Logistic Regression

Below is a brief introduction to Ordinal Logistic Regression [37], which serves as the foundation of our methodology.

Definition 2.1. (Proportional Odds Model). Given the ordinal category $k \in \{0, \dots, C\}$, the proportional odds model satisfies:

$$\log \frac{P(k \leq c | \mathbf{x})}{P(k > c | \mathbf{x})} = a_c - \beta^\top \mathbf{x}, \quad (1)$$

where k denotes an observed ordinal variable with C categories. \mathbf{x} denotes the covariate, and β represents the corresponding regression coefficients. The thresholds a_c determine when each level of the ordinal response variable becomes likely.

For each category c , the cumulative probability is defined as:

$$P(k \leq c | \mathbf{x}) = \sigma(a_c - \beta^\top \mathbf{x}) \quad (2)$$

where $\sigma(\cdot)$ represents the sigmoid function. Especially, $k = 0$ is a null category and we define $P(k \leq 0) = 0$. Additionally, we have $P(k \leq C) = 1$. As a result, the probability of predicting category $k = c$ is defined as:

$$P(k = c | \mathbf{x}) = P(k \leq c | \mathbf{x}) - P(k \leq c - 1 | \mathbf{x}) \quad (3)$$

According to the proportional odds assumption, the threshold parameters a_c are independent, but the regression coefficients β are shared across all categories. The loss function using Maximum Likelihood Estimation (MLE) to optimize the model is given by:

$$L = - \sum_{s=1}^S \sum_{c=1}^C I(k_s = c) \log P(k_s = c | \mathbf{x}_s)$$

where $I(k_s = c)$ is an indicator function and S is the size of samples.

3 METHODOLOGY

To effectively address the MFCF problem and overcome the limitations of prior works, we propose Generalized Neural Ordinal Logistic Regression (GNOLR) framework, comprising two key components: **(1) a mapping mechanism** that translates unstructured implicit feedback into structured, ordered categorical labels, and **(2) a generalized OLR model** with enhanced expressibility to capture complex relationships in implicit feedback.

3.1 Map Implicit Feedback To Ordinal Labels

To align implicit feedback with the ordinal label constraints of OLR while reflecting users' progressive engagement, we propose a label mapping mechanism comprising two steps: (1) *Sparsity-based Feedback Ordering* and (2) *Exclusive Ordinal Category Assignment*.

Step 1. Prior studies [11, 47, 53] suggest that feedback sparsity indicates the level of user preference: actions requiring greater commitment (e.g., purchases) occur less frequently but convey higher preference than more common actions (e.g., clicks). We thus arrange feedback signals in ascending order of occurrence frequency, i.e., signals with lower frequency yet higher preference come later.

Formally, consider T feedback types $Y = \{y_t\}_{t=1}^T$, where $y_t = 0$ denotes the absence of feedback (often treated as negative [34, 47, 50, 53, 62]). Let $pos(y_t)$ denote the number of samples in which $y_t = 1$. We reorder feedback types so that the index $i > j$ if $pos(y_i) < pos(y_j)$. This yields a new sequence $[y_1, \dots, y_T]$ in ascending order of sparsity (i.e., from the lowest preference to highest preference).

Step 2. Given above ordered feedback list, our goal is to map each sample's implicit signals to a *single* ordinal label k . Because implicit feedback may not follow a strict order and multiple feedback can be positive simultaneously (e.g., user can click and purchase an item without adding to cart), we select the *largest index of positive feedback* within the reordered list, indicating the highest engagement level is reached. Formally, this mapping is defined as:

$$k = \begin{cases} \max(\{t + 1 \mid y_t > 0\}), & \text{if } \exists y_t > 0, t \in [1, T] \\ 1, & \text{if } \forall t \in [1, T], y_t = 0. \end{cases}$$

Note that, by default, $P(k \leq 0) = 0$ for $k = 0$, to maintain the mathematical rigor of the formulation. $k = 1$ denotes the "no positive feedback" (impression) case. Overall, multiple feedback is mapped to one $k \in \{0, T + 1\}$, implying the ordinal user preference level.

Illustrative Example. Consider three implicit feedback signals: click (y_1), add to cart (y_2), and purchase (y_3). These events are naturally ordered by their sparsity as $[y_1, y_2, y_3]$. **Case 1:** If all three labels for an item i are 0 for a user u , it means u has only seen the item (impression) without taking any action. This state indicates the lowest engagement, and the mapped label is $k = 1$. **Case 2:** If u clicked on i and directly purchased it, we have $y_1 = 1$ and $y_2 = 0$, and $y_3 = 1$. Based on the mapping, $k = 4$, as purchase ($y_3 = 1$) represents the highest level of engagement and sparsity.

3.2 Generalize OLR with Nested Optimization

With the mapped ordinal labels, we generalize the standard OLR in two aspects to enhance its expressibility. First, we replace its linear formulation with Neural OLR [6] to model non-linear dependencies between covariants and labels. Second, we introduce a nested

optimization framework to capture the progressive structure of user-item interactions (see Figure 2).

3.2.1 Neural OLR for MFCF. To learn user- and item-specific embeddings for the MFCF problem, we adopt the Twin Tower architecture [25, 55, 57], in which separate neural encoders extract embeddings for users and items. Formally, let $f_u(\cdot)$ and $f_i(\cdot)$ denote neural encoders that map user and item features to their respective embeddings: $\mathbf{e}_u = f_u(\mathbf{x}_u)$ and $\mathbf{e}_i = f_i(\mathbf{x}_i)$, where \mathbf{x}_u and \mathbf{x}_i denote the raw user and item features (Figure 2). Under this setup, the Proportional Odds Model (Equation (1)) is reformulated as:

$$\log \frac{P(k \leq c \mid \mathbf{x}_u, \mathbf{x}_i)}{P(k > c \mid \mathbf{x}_u, \mathbf{x}_i)} = a_c - \mathcal{K}(\mathbf{e}_u, \mathbf{e}_i),$$

where \mathcal{K} is a kernel to measure similarity.

3.2.2 Nested Optimization Framework. With Neural OLR for greater flexibility, we now address its remaining limitation: **shared encoders** still restrict the model's ability to learn feedback-specific feature dependencies (Figure 2). A naive solution—training completely separate encoders for each feedback type—would fragment the embedding space. To address this issue, we propose a **Nested Optimization Framework** with two key components: *Nested Category-Specific Encoding* and *Nested OLR Optimization*:

(1) Nested Category-Specific Encoding is designed for category-aware feature extraction with separate encoders. Instead of generating a single user preference embedding directly, we construct a sequence of user-item embedding subspaces using multiple Twin Tower encoders. Each encoder captures a distinct level of user engagement, contributing to a progressively enriched representation.

Formally, consider we have T implicit feedback types, mapped into an ordinal category sequence $[0, 1, \dots, T + 1]$. Let (f_u^c, f_i^c) represent the neural encoders for each category $c \in [1, T]$, producing the embeddings: $(\mathbf{e}_u^c, \mathbf{e}_i^c) = (f_u^c(\mathbf{x}_u^c), f_i^c(\mathbf{x}_i^c))$ and are ℓ_2 -normalized. To get a **unified space**, we define the **Nested Embedding** as:

$$\mathbf{E}_u^c = \text{Concat}[\mathbf{e}_u^1, \dots, \mathbf{e}_u^c], \quad \mathbf{E}_i^c = \text{Concat}[\mathbf{e}_i^1, \dots, \mathbf{e}_i^c]$$

Each \mathbf{E}_u^c and \mathbf{E}_i^c aggregates representations from all preceding levels, ensuring all lower-order information is considered in predicting higher order categories. Note that category 0 and $T + 1$ do not require learned embeddings. Building upon nested embeddings, we generalize the proportional odds model (Equation (1)) as follows:

$$\log \frac{P(k \leq c \mid \mathbf{x})}{P(k > c \mid \mathbf{x})} = a_c - c\gamma\mathcal{K}(\mathbf{E}_u^c, \mathbf{E}_i^c), \quad (4)$$

where $\mathcal{K}(\mathbf{a}, \mathbf{b}) = \frac{\mathbf{a}^T \mathbf{b}}{\|\mathbf{a}\| \cdot \|\mathbf{b}\|}$ (Cosine) and γ is a reshaping factor controlling the output distribution of the kernel function. Following the cumulative probability formulation in Equation (2), we derive:

$$P(k \leq c \mid \mathbf{x}_u, \mathbf{x}_i) = \sigma(a_c - c\gamma\mathcal{K}(\mathbf{E}_u^c, \mathbf{E}_i^c)), \quad (5)$$

and thus the probability of predicting category $k = c$ becomes:

$$P(k = c \mid \mathbf{x}_u, \mathbf{x}_i) = \sigma(a_c - c\gamma\mathcal{K}(\mathbf{E}_u^c, \mathbf{E}_i^c)) - \sigma(a_{c-1} - (c-1)\gamma\mathcal{K}(\mathbf{E}_u^{c-1}, \mathbf{E}_i^{c-1})) \quad (6)$$

Here, a_c and a_{c-1} act as constants in the OLR paradigm. By leveraging the monotonicity of the sigmoid (σ), maximizing $P(k = c \mid \mathbf{x}_u, \mathbf{x}_i)$ effectively pushes $\mathcal{K}(\mathbf{E}_u^{c-1}, \mathbf{E}_i^{c-1})$ and $\mathcal{K}(\mathbf{E}_u^c, \mathbf{E}_i^c)$ apart. If \mathbf{e}_u^c and \mathbf{e}_i^c are ℓ_2 -normalized and \mathcal{K} is cosine, then when the user's preference level truly reaches category c , the model promotes **similarity** in the preceding sub-embeddings \mathbf{E}_u^{c-1} and \mathbf{E}_i^{c-1} (lower-level

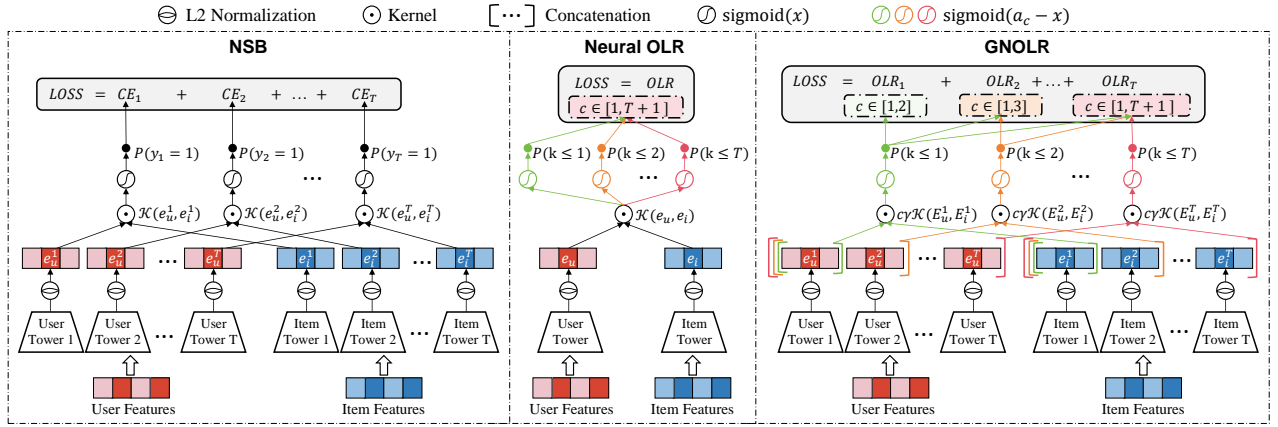


Figure 2: Comparison of three architectures. NSB (left) represents the predominant collaborative filtering framework for multiple implicit feedback signals, known as Naive Shared Bottom, which models each task independently. Neural OLR (middle) extends OLR to neural modeling using a shared encoder. GNOLR (right) further generalizes OLR with nested encoding and subtasks to enhance expressibility and unify the embedding of user engagement across tasks.

categories) and enforces **dissimilarity** in e_u^c and e_i^c . Consequently, e_u^c and e_i^c contribute positively only if the user reaches a higher preference level than c , effectively acting as a "goalkeeper". In other words, each higher-level embedding is "activated" only after the user preference has surpassed the corresponding threshold.

Further, note that $P(k > T | \mathbf{x}_u, \mathbf{x}_i)$ can be written as $1 - P(k \leq T | \mathbf{x}_u, \mathbf{x}_i) = 1 - \sigma(a_T - \gamma \sum_{c=1}^T \mathcal{K}(e_u^c, e_i^c))$, implying an aggregation of all preference-level information. Thus $P(k > T | \mathbf{x}_u, \mathbf{x}_i)$ is also interpreted as the **unified preference score**, and E_u^T, E_i^T are the **unified preference embeddings**, where higher similarity between them indicates a higher preference level.

(2) **Nested OLR Optimization.** Standard OLR assigns each sample to exactly one category. However, maximizing $P(k = c)$ alone does not ensure a progressive probability distribution for the preceding categories. For instance, consider three categories ($k \leq 3$) and following scenarios. Scenario A: $P(k = 1) = 0.4, P(k = 2) = 0, P(k = 3) = 0.6$ and Scenario B: $P(k = 1) = 0.1, P(k = 2) = 0.3, P(k = 3) = 0.6$. They all produce $P(k = 3) = 0.6$ but only Scenario B reflects a user's ideal preference distribution who just surpasses preference level 2 but not exceeds level 3.

To stabilize learning and ensure each category's probability aligns with ideal user's engagement progression, we propose a Nested OLR Optimization framework. Specifically, we define T subtasks, each focusing on a partial view of the category space. For subtask $t \leq T$, we consider only categories $\{0, \dots, t+1\}$. Any sample with an assigned category $k < t+1$ retains its label, while any sample with a label $k \geq t+1$ is re-labeled to $t+1$. This merges higher categories into one, ensuring subtask t focuses probability distribution among the preceding levels ($k \leq t+1$), namely *category remapping*. Let k_s^t be the re-mapped category of sample s for subtask t . Using the probabilities from Equation (6), the overall loss is:

$$L = \sum_{t=1}^T L_t, \quad L_t = -\sum_{s=1}^S \sum_{c=1}^{t+1} I(k_s^t = c) \log P(k_s^t = c | \mathbf{x}_u^s, \mathbf{x}_i^s),$$

By optimizing all subtasks jointly, the model is encouraged to distribute probabilities appropriately across all categories. We refer to this entire framework as **Generalized Neural OLR (GNOLR)**.

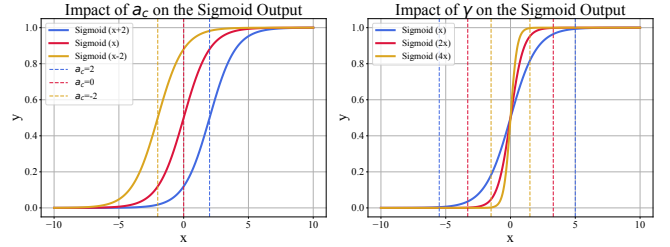


Figure 3: The impact of a_c and γ on Sigmoid predictions. a_c shifts the Sigmoid curve horizontally. γ modifies the steepness of the Sigmoid curve, controlling which region of the input space receives greater focus during learning.

3.3 Compare with Feedback-Wise Modeling

Predominant approaches [23, 34, 47, 50, 62] commonly model multiple implicit feedback signals by optimizing a set of binary classification tasks using **Cross-Entropy (CE)** loss. In this section, we theoretically demonstrate why GNOLR offers advantages over these approaches by comparing GNOLR with standard CE.

3.3.1 Single Feedback Case. Here we show GNOLR's mathematical equivalence to CE loss while $\{a_c\}$ and γ enhance adaptability. Consider we only have clicks as feedback. Through mapping, we derive three categories $k \in \{0, 1, 2\}$ where $k = 1$ denotes no interaction, and $k = 2$ is a click. By definition, $I(k = 1) = 1 - I(k = 2)$. Under this setup, the GNOLR loss can be expressed as: $L = -\sum_{s=1}^S \sum_{c=1}^2 I(k_s = c) \log P(k_s = c | \mathbf{x}_u^s, \mathbf{x}_i^s)$. Expand $P(k_s = c)$ and let $y = I(k_s = 2)$, the loss for sample s becomes:

$$L = -(1-y) \log \sigma(a_1 - \gamma \mathcal{K}(e_u, e_i)) - y \log(1 - \sigma(a_1 - \gamma \mathcal{K}(e_u, e_i)))$$

Rewriting with $\sigma(x) = 1 - \sigma(-x)$, we have:

$$L = -(1-y) \log(1 - \sigma(\gamma \mathcal{K}(e_u, e_i) - a_1)) - y \log(\sigma(\gamma \mathcal{K}(e_u, e_i) - a_1)).$$

This is equivalent to the CE loss. However, the key distinction is that GNOLR introduces two key parameters a_1 and γ which changes the output distribution of the Cosine kernel. From the perspective

of CE loss, the threshold a_1 ensures that the model predicts high probability only when $\gamma\mathcal{K}(\mathbf{e}_u, \mathbf{e}_i)$ exceeds a_1 . This mechanism effectively pulls user and item embeddings closer for positive pairs, enhancing nearest neighbor retrieval. Additionally, γ controls the scaling of $\mathcal{K}(\mathbf{e}_u, \mathbf{e}_i)$, thereby influencing the range of inputs that receive significant gradient updates. As a result, adjusting γ shifts the model’s focus toward different sample distributions, improving adaptability to varying levels of difficulty in the data.

This reformulation reveals that GNOLR enhances model’s flexibility and adaptability over standard CE by shifting the impact and reshaping the σ ’s output distribution with a_c and γ . The impact of a_c and γ on the prediction distribution is illustrated in Figure 3.

3.3.2 Multi-Feedback Case. Here we show that GNOLR avoids contradictory label assignments in multi-feedback CE loss by modeling multi-level feedback in a unified and consistent manner. For simplicity, consider a scenario with two feedback: clicks and purchases (pay). We define a category list $k \in [0, 1, 2, 3]$, where $k = 0$ is null, $k = 1$ means no feedback, $k = 2$ means clicked but unpaid, $k = 3$ means paid. Through the eyes of prior multi-task frameworks [23, 34, 47], we can interpret the category indicators as: $I(k = 1) = 1 - y_{click}$, $I(k = 2) = \max(y_{click} - y_{pay}, 0)$, and $I(k = 3) = y_{pay}$. Here, y_{click} and y_{pay} are binary indicators for click and purchase, respectively. Similarly, we can infer the predicted probabilities for each category as: $p(k = 1 | \mathbf{x}) = 1 - p_{ctr}$, $p(k = 3 | \mathbf{x}) = p_{ctcvr}$, and thus $p(k = 2 | \mathbf{x}) = p_{ctr} - p_{ctcvr}$, where p_{ctr} is the predicted Click-Through Rate (CTR), and p_{ctcvr} is the predicted Purchase Rate (CTCVR). The loss function for a single sample under GNOLR can then be expands to:

$$L = -2(1 - y_{click}) \log(1 - p_{ctr}) - y_{click} \log p_{ctr} - y_{pay} \log p_{ctcvr} - \max(y_{click} - y_{pay}, 0) \log(p_{ctr} - p_{ctcvr}) \quad (7)$$

In feedback-wise approaches (using separate CE loss for each feedback) [23, 34, 47, 50, 62], a CTR head is used to predict p_{ctr} , and a CTCVR head predicts p_{ctcvr} . Although the first line in Equation (7) appear in feedback-wise CE loss, a crucial difference lies in how clicked and unpurchased samples ($y_{click} = 1, y_{pay} = 0$) are treated. CE loss uniformly pushes p_{ctcvr} to 0 for all unpurchased samples, while increasing p_{ctr} to 1 for all clicked items, which may lead to inconsistent supervision signals between the CTR and CTCVR heads. By contrast, GNOLR avoids explicitly assigning such conflicting targets to clicked-but-unpurchased items, and instead emphasizes the relative difference between p_{ctr} and p_{ctcvr} , potentially leading to more coherent learning dynamics.

3.4 Manual Ordinal Thresholds Selection

In conventional OLR, the thresholds $\{a_c\}$ follow an inherent order: $a_1 < a_2 < \dots < a_T$ and can be learned jointly with the model. However, GNOLR’s nested optimization framework may disrupt this ordering. To resolve this, we propose a novel approach to directly compute a near-optimal ordinal set $\{a_c\}$, eliminating the need for hyperparameter tuning. Specifically, we calculate $\{a_c\}$ by: $a_c \approx \log \frac{1 - \mathbb{E}[P(k > c | \mathbf{x})]}{\mathbb{E}[P(k > c | \mathbf{x})]}$, where $\mathbb{E}[P(k > c | \mathbf{x})]$ denotes the sample proportion of instances belonging to categories strictly above c . This quantity is straightforward to compute from the data.

Specifically, given that cosine similarity is symmetric and bounded in $[-1, 1]$, we encourage $\mathbb{E}_{\mathbf{x}}[\mathcal{K}(E_u, E_i)] \approx 0$ for balanced similarity distribution. For category c , the OLR-based formulation implies

Table 1: Statistics of all datasets. The number of users and items in the AE series datasets is not disclosed. #Pos₁ and #Pos₂ denotes the counts for click and pay in e-commercial datasets, likes and follows for video datasets.

Dataset	#User	#Item	Total	#Pos ₁	#Pos ₂
Ali-CCP	0.24M	0.47M	69.1M	2.62M	13.1K
AE-ES	/	/	31.67M	0.84M	19.1K
AE-FR	/	/	27.04M	0.54M	14.4K
AE-NL	/	/	7.31M	0.17M	6K
AE-US	/	/	27.39M	0.45M	10.8K
KR-Pure	24.9K	6.8K	0.92M	19.78K	1.13K
KR-1K	1K	2.4M	6.75M	0.13M	7.98K
ML-1M	6K	3.7K	1M	0.23M	/
ML-20M	138K	27K	20M	4.43M	/
RetailR	1.4M	0.24M	2.76M	91.8K	22.5K

$\log \frac{1 - P(k > c | \mathbf{x})}{P(k > c | \mathbf{x})} = a_c - c\gamma\mathcal{K}(E_u^c, E_i^c)$. Taking expectations over \mathbf{x} and applying Jensen’s inequality for approximation gives:

$$\mathbb{E}[a_c - c\gamma\mathcal{K}(\mathbf{e}_u, \mathbf{e}_i)] = \mathbb{E}\left[\log \frac{1 - P(k > c | \mathbf{x})}{P(k > c | \mathbf{x})}\right] \geq \log \mathbb{E}\left[\frac{1 - P(k > c | \mathbf{x})}{P(k > c | \mathbf{x})}\right]$$

$$a_c \approx \log \mathbb{E}\left[\frac{1 - P(k > c | \mathbf{x})}{P(k > c | \mathbf{x})}\right] \approx \log \frac{1 - \mathbb{E}[P(k > c | \mathbf{x})]}{\mathbb{E}[P(k > c | \mathbf{x})]}$$

Because our label mapping orders implicit feedback signals in ascending order of sparsity, the thresholds $\{a_c\}$ estimated via this approach naturally form an increasing sequence. In practice, **manually setting these thresholds often stabilizes training**, and we observe that thresholds obtained via learning are typically close to the values derived from the above empirical approximation.

4 EXPERIMENTS

In the context of embedding-based collaborative filtering, an effective algorithm should achieve two objectives: **(1) align spatial proximity with user interest**, ensuring that similar user-item pairs are closer in the embedding space, and **(2) provide strong personalized ranking capabilities**, displaying items with higher engagement propensity at higher-ranked positions in the list. In this section, we conduct extensive experiments on nine public real-world datasets to address the following research questions:

- **RQ1** How does GNOLR perform on single-task and multi-task ranking compared to state-of-the-art (SOTA) methods?
- **RQ2** How does GNOLR perform on the embedding-based collaborative filtering (retrieval) task relative to the baselines?
- **RQ3** How does GNOLR deal with prevalent listwise modeling?
- **RQ4** How sensitive is GNOLR to the hyper-parameter settings?
- **RQ5** How much does the Nested Optimization Framework contribute to GNOLR’s performance?

4.1 Experiment Setup

4.1.1 Datasets. To comprehensively evaluate GNOLR, we use nine widely-adopted, large-scale, and real-world datasets spanning diverse recommendation scenarios and task settings: **(1) Ali-CCP** [34]: An e-commerce dataset from Taobao’s recommender system, containing two implicit feedback types (click and pay). To align with the collaborative filtering setup, we discard user-item cross features and use only user-side and item-side features. **(2) AE** [30]: An e-commerce dataset from AliExpress’s search logs, with four

Table 2: Single-Task Ranking Results (AUC). Methods predict the probability of clicks for Ali-CCP and AE, predict likes for KuaiRand, ATC for RetailRocket, and predict positive for the MovieLens datasets. The best results (statistically significant) are highlighted in bold, while the second-best results are underlined.

Method	BCE	BCE*	JRC	JRC*	GNOLR
AliCCP	0.5005	0.5896	0.5009	<u>0.5924</u>	0.6232
AE-ES	0.5078	0.7118	0.6323	<u>0.7357</u>	0.7366
AE-FR	0.5008	0.6887	0.6428	<u>0.7307</u>	0.7335
AE-US	0.5078	0.6165	0.6256	<u>0.6831</u>	0.7062
AE-NL	0.5155	0.6715	0.6419	<u>0.6853</u>	0.7298
KR-Pure	0.6056	0.7665	0.7835	<u>0.8280</u>	0.8506
KR-1K	0.7485	0.8510	0.8018	<u>0.8684</u>	0.9024
ML-1M	0.7542	0.7896	0.7937	<u>0.7939</u>	0.8139
ML-20M	0.7535	0.7790	0.7801	<u>0.7854</u>	0.8094
RetailR	0.5034	<u>0.7308</u>	0.5009	0.7165	0.7537

Table 3: The GAUC performance comparison of various ranking methods across multiple datasets. The best results (statistically significant) are highlighted in bold, while the second-best are underlined. λ Rank is LambdaRank.

Dataset	RankNet	λ Rank	ListNet	S2SRank	SetRank	JRC	GNOLR _L
AliCCP	0.5518	<u>0.5534</u>	0.5447	0.5499	0.5523	0.5009	0.5602
AE-ES	<u>0.5432</u>	0.5426	0.5431	0.5421	0.5403	0.5236	0.5433
AE-FR	<u>0.5351</u>	0.5343	0.5338	0.5347	0.5331	0.5159	0.5364
AE-US	<u>0.5294</u>	0.5291	0.5289	0.5287	0.5273	0.5159	0.5300
AE-NL	<u>0.5278</u>	0.5270	0.5272	0.5275	0.5274	0.5201	0.5346
KR-Pure	<u>0.5090</u>	0.5073	0.5075	0.5079	0.5106	0.5082	0.5084
KR-1K	0.5062	0.4953	0.5084	0.5136	<u>0.5242</u>	0.5036	0.5380
ML-1M	<u>0.7121</u>	0.6891	0.6985	0.7057	0.6974	0.7040	0.7244
ML-20M	0.6941	<u>0.6869</u>	0.6969	0.6874	0.6730	0.6817	0.7006

sub-datasets from different country markets (AE-ES, AE-FR, AE-NL, AE-US). Each sub-dataset includes click and pay feedback. (3) **KuaiRand** [13]: A video recommendation dataset from the Kuaishou app. We use two versions (KR-Pure, KR-1K) of it, differing by their user and item sampling strategies. Two types of implicit feedback, likes and follows, are used in modeling. (4) **RetailRocket**: A dataset from a real-world e-commerce website, containing three types of user behaviors: click, add-to-cart (ATC), and Pay. We use the latter two. (5) **MovieLens** [17]: A widely used movie recommendation dataset, with two versions (ML-1M, ML-20M). We set a rating threshold (> 4) to create binary labels to simulate implicit feedback. To simulate real-world scenarios, we sort all samples chronologically and split the data into 70% (history) for training and 30% (future) for testing. The statistics are listed in Table 1.

4.1.2 Evaluation Metrics. We use the following metrics for different problems. For RQ1, RQ3, and RQ4, we use the widely adopted AUC (Area Under the ROC Curve) [23, 34, 47, 50, 62]. For RQ3, we add the GAUC (AUC averaged over user sessions) [18, 61] to measure listwise performance. For RQ2, we use Recall@K [24, 51, 58], where each user’s candidate items are ranked by Euclidean distance between user and item embeddings, and the proportion of positive items (of corresponding targets) in the top K is calculated.

4.1.3 Baselines. We use state-of-the-art methods as baselines across different task settings: For RQ1, we consider Binary Cross Entropy (BCE) and JRC [43] as single-task baselines. For multi-task settings, we include NSB (Naive Shared Bottom), ESMM [34], ESCM²-IPS [50], ESCM²-DR [50], DCMT [62], NISE [23], and TAFE [47]. For RQ2, all pointwise, pairwise, listwise, or setwise ranking methods are suitable for **single-task** personalized retrieval, as they all focus on distinguishing positive samples from negatives for each user. We evaluate BCE, RankNet [1], LambdaRank [3], ListNet [4], SetRank [49], S2SRank [5], and JRC [43]. However, for **multi-task** personalized retrieval, none of the existing SOTA multi-task methods can generate retrieval-oriented embeddings for all tasks. For instance, ESMM models ctrcvr as the product of ctr and cvr, thus the embeddings from the cvr encoder cannot be used for ctrcvr-oriented retrieval. Therefore, we only compare GNOLR with NSB, as it directly associates its embeddings with corresponding labels. For RQ3, we include: RankNet [1], LambdaRank [3], ListNet [4], SetRank [49], S2SRank [5], and JRC [43].

Methods marked with "*" indicate that they were fine-tuned with a **sample reweighting** technique [16, 32]. Specifically, we only increase the weight of positive samples for each feedback.

4.1.4 Implementations. To ensure a fair comparison, all methods use the same backbone network architecture: **Twin Tower encoders with standard MLPs** [25]. Additionally, all embeddings are ℓ_2 -normalized to facilitate compatibility with nearest neighbor search in the Euclidean space [24, 55]. Hyper-parameters for each method are tuned independently (grid-search) for each dataset to achieve optimal performance (see Appendix for details). The reported results represent the average of ten independent runs. **Our code** is available at <https://github.com/FuCongResearchSquad/GNOLR>.

4.2 Results and Analysis

4.2.1 RQ1: Ranking Performance. Table 2 and Table 4 present the ranking performance of various methods under single-task and multi-task settings. We have the following observations:

(1) **Overall Gains.** GNOLR demonstrates superior performance consistently across both single-task and multi-task settings. Its ability to model complex user preferences and leverage additional implicit signals effectively is evident from its significant improvements over the baselines. Notably, the progression of user engagement is captured effectively in different recommendation contexts (e.g., e-commerce, movie, and short video recommendation).

(2) **Robustness to Extremely Imbalanced Distribution.** GNOLR maintains strong performance on highly imbalanced e-commerce datasets (e.g., Ali-CCP, AE), where baselines often fail (AUC ≈ 0.5). This is due to cross-entropy loss struggles with such imbalanced distributions [31]. While **sample reweighting** improves baselines’ performance, GNOLR outperforms them **without** requiring such adjustments. This advantage stems from GNOLR’s structured label hierarchy, which models feedback progression instead of dealing with them independently. Additionally, GNOLR sets a_c directly based on label distribution, avoiding tuning, while γ enables hard sample mining. These hyperparameters adaptively adjust GNOLR’s prediction distributions and further enhance robustness.

Table 4: Multi-Task Ranking Results (AUC). The best results are highlighted in bold, while the second-best are underlined.

Task	Dataset	NSB*	ESMM*	ESCM ² -IPS*	ESCM ² -DR*	DCMT*	NISE*	TAFE*	Neural OLR	GNOLR
CTR	AliCCP	0.5877	0.5955	0.5947	0.5962	0.5952	0.6020	0.5981	0.6162	<u>0.6153</u>
	AE-ES	0.7024	0.7084	<u>0.7337</u>	0.7271	0.6963	0.7079	0.7089	0.7257	0.7372
	AE-FR	0.7103	0.6798	<u>0.7322</u>	0.7156	0.6714	0.6932	0.6959	0.7194	0.7370
	AE-US	0.6415	0.6593	0.6837	0.7014	0.6513	0.6735	0.6751	0.6792	0.6971
	AE-NL	0.6505	0.6903	0.6656	0.6706	0.6621	0.6882	0.6975	0.6563	0.7277
CTCVR	AliCCP	0.5070	0.5453	0.5439	<u>0.5527</u>	0.5412	0.5351	0.5336	0.5362	0.5997
	AE-ES	0.7150	0.8433	0.8439	<u>0.8563</u>	0.8483	0.8143	0.8139	0.7858	0.8827
	AE-FR	0.7262	0.8219	0.8274	0.8565	<u>0.8610</u>	0.7797	0.7874	0.7618	0.8793
	AE-US	0.6850	0.8237	0.7820	<u>0.8403</u>	0.8221	0.7719	0.7820	0.7354	0.8663
	AE-NL	0.7143	<u>0.8129</u>	0.7808	0.7986	0.8051	0.7601	0.7801	0.7379	0.8343
Like	KR-Pure	0.8077	0.8157	0.8077	0.8124	0.8250	0.8271	0.8286	<u>0.8440</u>	0.8456
	KR-1K	0.8865	0.8817	0.8892	0.8858	0.8794	0.8816	0.8890	<u>0.9079</u>	0.9087
Follow	KR-Pure	0.7025	0.6994	0.6909	0.7025	0.7056	0.6994	0.6963	0.7212	<u>0.7161</u>
	KR-1K	0.7318	0.7399	<u>0.8113</u>	0.7888	0.7999	0.6868	0.7327	0.7100	0.8165
ATC	RetailR	0.6845	0.6981	0.6912	0.6926	0.6942	0.6945	0.7013	<u>0.7521</u>	0.7764
Pay	RetailR	0.7247	0.8148	0.8209	0.8139	0.8150	<u>0.8238</u>	0.7868	0.8189	0.8242

(3) **Prior Limitation in Task Balancing.** Even after applying sample re-weighting, the baselines remain inferior to GNOLR. This can be attributed to the **potential conflicts** induced by the feedback-wise formulation, which increase the difficulty of finding a robust Pareto frontier of task-specific weights for prior frameworks [40]. Consequently, these methods suffer from **gradient conflicts** arising from improper label modeling, as discussed in Section 3.3.

(4) **Impact of Minority Category.** GNOLR shows minor performance variations when transitioning from single-task to multi-task prediction. For instance, the AUC for click prediction on AliCCP drops from 0.6232 to 0.6153, while it improves from 0.7335 to 0.7370 on AE-FR. Generally, we expect GNOLR to improve as more implicit feedback signals are incorporated, as they provide richer information about user preferences. However, the minor performance drop in some cases, such as AliCCP, may be attributed to the sparsity of certain interactions, since GNOLR shows uplift on dense-interacted datasets like AE-ES and AE-FR. Sparse positive feedback can lead to **insufficient distribution fitting** near the ordinal category boundaries ($\{a_c\}$). Addressing this limitation is left for future work.

4.2.2 **RQ2: Retrieval Performance.** The results of single- and multi-task retrieval are presented in Tables 5 and 6. GNOLR demonstrates superior performance in both single-task and multi-task retrieval tasks. Key observations are as follows.

(1) **Adaptability to Imbalanced Data.** GNOLR’s advantage in single-task retrieval arises from its adaptability to imbalanced distributions. The hyperparameter γ reshapes the sigmoid curve to emphasize challenging samples, while a_c shifts the curve, refining the boundary between positive and negative items. These adjustments yield a more coherent embedding space topology with the data distribution and thus stronger retrieval performance.

(2) **Unified Embedding for Multi-Target Retrieval.** In multi-task retrieval, GNOLR significantly outperforms NSB* (NSB with reweighting), especially on sparse targets. Unlike NSB*’s task-specific embeddings, GNOLR employs a unified embedding space, enabling retrieval across multiple feedback signals with **the same set of**

embeddings. Conventional methods fail to capture label correlations, particularly the progressiveness of user interest. This results in disjoint embedding spaces and lower recall when applying one task’s embedding to another, e.g., evaluating embedding NSB_{follow} on the "like" target will lead to drop in Recall. GNOLR’s unified framework avoids this pitfall by leveraging the **category-specific nested optimization** framework (Figure 2) among tasks.

(3) **Spatial Structure Visualization.** The superiority of GNOLR in retrieval is illustrated in the visualization (Figure 4). For single-task settings, embeddings trained with standard CE loss exhibit a poor discriminative topology: the angle between the user vector and positive item vectors often exceeds 90° , making nearest neighbor retrieval less effective. In contrast, GNOLR adjusts the angle distribution through a_c , ensuring positive items form smaller angles with the user vector, thereby improving retrieval performance.

For multi-task settings, especially with sparse positive labels, CE loss often pushes all items away from the user vector, resulting in a "vacant" region within the half ball centered with the user vector (Figure 4-2(c)). This compressed embedding space reduces the model’s robustness to unseen data. GNOLR addresses this by shifting decision boundaries among categories towards user vectors according to their preference levels (achieved by proper configuration of $\{a_c\}$), ensuring robustness and improving retrieval performance, particularly for sparse targets.

4.2.3 **RQ3: Co-training with Listwise Loss.** Standard GNOLR primarily falls under pointwise ranking paradigm, but its personalization ability can be further enhanced by combining it with a listwise loss, such as ListNet [4]. Specifically, the combined loss is defined as $L = L_{GNOLR} + L_{ListNet}$, referred to as GNOLR_L. The results are shown in Table 3, and the following observations are made: (1) GNOLR_L outperforms the baselines on most datasets, demonstrating its ability to effectively integrate listwise learning into its framework. (2) GNOLR’s strength in pointwise ranking enhances the effectiveness of listwise learning. For example, when combined with ListNet, GNOLR significantly improves both AUC

Table 5: Single-Task Retrieval on ML-1M. The best result are presented in bold font, while the second-best are underlined.

Method	Recall@5	Recall@10	Recall@15	Recall@20
BCE	0.3890	0.5842	0.6939	0.7639
RankNet	<u>0.4011</u>	<u>0.6007</u>	<u>0.7110</u>	<u>0.7807</u>
LambdaRank	0.3924	0.5884	0.6981	0.7672
ListNet	0.3903	0.5927	0.7015	0.7704
SetRank	0.3931	0.5922	0.7032	0.7725
S2SRank	0.3967	0.5966	0.7077	0.7768
JRC	0.3684	0.5739	0.6860	0.7579
GNOLR	0.4086	0.6090	0.7182	0.7865

Table 6: Multi-Target Retrieval on KR-1K. Best in bold font. NSB*_{like} denotes embeddings from the "like" encoder.

Target	Model	Recall@50	Recall@100	Recall@200	Recall@500
Like	NSB* _{like}	0.0583	0.1024	0.1809	0.3604
	NSB* _{follow}	0.0453	0.0911	0.1672	0.3312
	GNOLR	0.0586	0.1085	0.1957	0.3841
Follow	NSB* _{like}	0.0301	0.0614	0.1239	0.2512
	NSB* _{follow}	0.0331	0.0768	0.1429	0.2710
	GNOLR	0.0419	0.0832	0.1529	0.2966

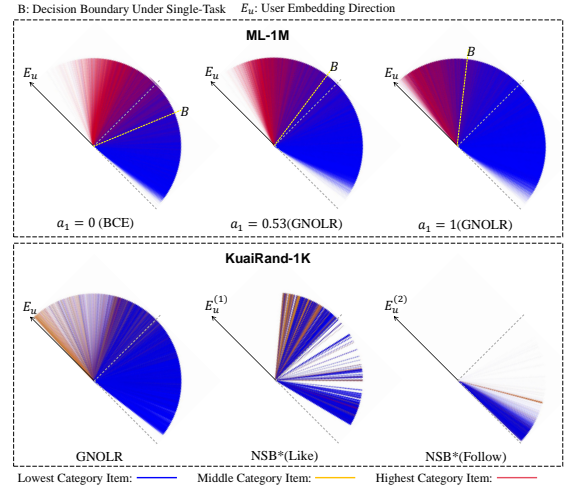
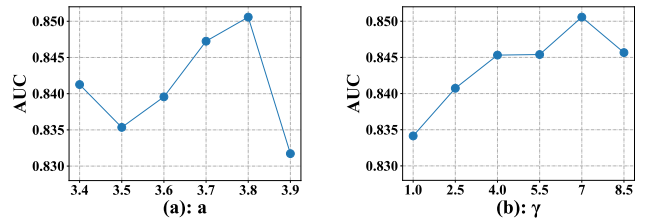
Table 7: Ablation Study on two representative datasets.

Dataset	Task	Neural OLR	GNOLR-V0	GNOLR-V1	GNOLR
Ali-CCP	CTR	0.6114	0.6041	0.5965	0.6085
	CTCVR	0.5221	0.5883	0.5854	0.6163
KR-1K	Like	0.9061	0.9023	0.9047	0.9079
	Follow	0.7106	0.6815	0.8076	0.8163

and GAUC compared to ListNet. (3) GNOLR_L achieves substantially better performance than JRC [43], a method specifically designed to balance calibration (AUC) and personalization (GAUC), indicating GNOLR_L's versatility and superior ranking ability in diverse scenarios (See AUC results in Appendix). Note that GAUC is not reported for RetailRocket in the main results, as most users interact with only one item, making personalization effects unobservable; AUC is still provided in the Appendix for reference.

4.2.4 RQ4: Parameter Sensitivity. We perform parameter sensitivity experiments to analyze the impact of key architectural and optimization parameters on GNOLR's performance. Overall, GNOLR is robust to most hyperparameters, with the exception of a (category thresholds) and γ (reshaping factor), which have more impact on performance. The results are presented in Figure 5. Notably, the optimal value of a aligns closely with the calculation detailed in Section 3.4, confirming the theoretical basis for its selection.

4.2.5 RQ5: Ablation Study. The performance of Naive Neural OLR serves as an ablation baseline to evaluate the impact of GNOLR's task-specific encoder architecture (Figure 2). While Naive Neural OLR can occasionally achieve comparable or superior performance on the denser targets, it often suffers from significant degradation on the sparser ones. In contrast, GNOLR consistently delivers balanced performance across all targets. This is attributed to its task-specific encoder design, which selectively models the


Figure 4: Visualization of the angular distribution between user and item embeddings under single- and multi-task settings. We fix the user directions and plot item directions. NSB* uses sample re-weighting for better performance.

Figure 5: Parameter sensitivity w.r.t. a and γ on KR-Pure.

dependencies between categories and covariates. For Naive Neural OLR, the coefficients are dominated by the correlations between dense label and covariates. Notably, we use a "wider" MLP for Naive Neural OLR to ensure fairness in the total number of parameters.

To further validate the design of GNOLR, we implemented two variants of our GNOLR, i.e., GNOLR-V0 (replaces the shared encoder in Neural OLR with task-specific encoder) and GNOLR-V1 (only incorporating the Nested Category-specific Encoding). As shown in Table 7, Nested Category-specific Encoding significantly improves performance on sparse targets, and its combination with Nested OLR Optimization achieves the highest gain, demonstrating the effectiveness of the Nested Optimization Framework.

Additional results and analyses are provided in the Appendix.

5 RELATED WORK

Collaborative filtering (CF) [19, 21, 45] leverages collective user feedback to recommend relevant items, traditionally via neighborhood-based approaches [42] or matrix factorization [27]. However, these shallow models can struggle with complex data. In contrast, embedding-based deep CF—often implemented via a twin-tower model [25, 55, 57]—learns user and item embeddings separately and uses their

similarity as scores. For large-scale retrieval, approximate nearest neighbor search [10] provide efficient indexing, making this approach both robust and scalable for personalized retrieval.

Ordinal Logistic Regression (OLR) models ordinal categories by estimating cumulative probabilities [37]. Enhanced variants (e.g., generalized or partial proportional odds models [39, 48, 52]) allow category-specific effects, and neural OLR further extends learning capacity [36]. Researchers initially applied OLR to explicit ordered feedback in recommender systems [22]. Later work adapted OLR for implicit signals, for instance by grouping positive feedback for each item to form ordered labels [38] or designing generalized OLR for sparse targets [9]. However, both works can only deal with single feedback. No existing methods address the modern large-scale challenge as GNOLR tackles—unifying multiple implicit feedback types to capture global user preference.

Learning to Rank (LTR) trains models to order items by user preference or relevance, commonly used in search engines and recommender systems. LTR methods generally fall into three categories: (1) Pointwise methods [29] predict a relevance score for each user-item pair independently and potentially overlooks relative relationships among items. (2) Pairwise methods [1–3] compares sample pairs to determine which item in a pair is more relevant, thereby directly modeling relative ranking. (3) Listwise methods [4, 54] optimize the entire list’s ranking order (items displayed in a user session or under a query can be viewed as a list), aiming to place positive items at higher positions in a global scope.

Multi-Task Recommendation. Modern recommender systems often aim to optimize multiple objectives (e.g., click, purchases) simultaneously. Early approaches trained separate models per task, combining outputs via fusion layers, but struggled with label inconsistencies and missed task inter-dependencies. Some Multi-task learning (MTL) methods focus on strict causal dependencies like [34, 50, 62], while others focus on architecture innovation like [11, 33, 46, 47, 53]. Nonetheless, most methods still treat each task independently, missing the progressive nature of user behaviors.

6 CONCLUSION

This paper introduces GNOLR, a versatile embedding-based collaborative filtering methods, including a mapping technique to transform multiple implicit feedback to ordinal categories and a novel category-specialized nested encoding framework to model the progression of user engagement into a unified space. Theoretical comparisons highlight GNOLR’s commonality with, and strengths over, prior paradigms. Extensive experiments confirm GNOLR’s efficiency, adaptability, and robustness, outperforming state-of-the-art methods in diverse settings.

ACKNOWLEDGMENTS

This paper is partially supported by National Natural Science Foundation of China (NO. U23A20313, 62372471) and The Science Foundation for Distinguished Young Scholars of Hunan Province (NO. 2023JJ10080)

REFERENCES

- [1] Chris Burges, Tal Shaked, Erin Renshaw, Ari Lazier, Matt Deeds, Nicole Hamilton, and Greg Hullender. 2005. Learning to rank using gradient descent. In *Proceedings of the 22nd International Conference on Machine Learning*. 89–96.

- [2] Christopher JC Burges. 2010. From ranknet to lambdarank to lambdamart: An overview. *Learning* 11, 23-581 (2010), 81.
- [3] Christopher J. C. Burges, Robert Ragno, and Quoc Viet Le. 2006. Learning to rank with nonsmooth cost functions. In *Proceedings of the 20th International Conference on Neural Information Processing Systems*. 193–200.
- [4] Zhe Cao, Tao Qin, Tie-Yan Liu, Ming-Feng Tsai, and Hang Li. 2007. Learning to rank: from pairwise approach to listwise approach. In *Proceedings of the 24th International Conference on Machine Learning*. 129–136.
- [5] Lei Chen, Le Wu, Kun Zhang, Richang Hong, and Meng Wang. 2021. Set2setRank: Collaborative Set to Set Ranking for Implicit Feedback based Recommendation. In *Proceedings of the 44th International ACM SIGIR Conference on Research and Development in Information Retrieval*. 585–594.
- [6] Jianlin Cheng, Zheng Wang, and Gianluca Pollastri. 2008. A neural network approach to ordinal regression. In *2008 IEEE international joint conference on neural networks (IEEE world congress on computational intelligence)*. 1279–1284.
- [7] Paul Covington, Jay Adams, and Emre Sargin. 2016. Deep Neural Networks for YouTube Recommendations. In *Proceedings of the 10th ACM Conference on Recommender Systems*. 191–198.
- [8] Anirban Dasgupta, Ravi Kumar, and Tamas Sarlos. 2011. Fast locality-sensitive hashing. In *Proceedings of the 17th ACM SIGKDD International Conference on Knowledge Discovery and Data Mining*. 1073–1081.
- [9] Gregory Faletto and Jacob Bien. 2023. Predicting rare events by shrinking towards proportional odds. In *Proceedings of the 40th International Conference on Machine Learning*. 9547–9602.
- [10] Cong Fu, Changxu Wang, and Deng Cai. 2022. High Dimensional Similarity Search With Satellite System Graph: Efficiency, Scalability, and Unindexed Query Compatibility. *IEEE Transactions on Pattern Analysis and Machine Intelligence* 44, 8 (2022), 4139–4150.
- [11] Cong Fu, Kun Wang, Jiahua Wu, Yizhou Chen, Guangda Huzhang, Yabo Ni, Anxiang Zeng, and Zhiming Zhou. 2024. Residual Multi-Task Learner for Applied Ranking. In *Proceedings of the 30th ACM SIGKDD Conference on Knowledge Discovery and Data Mining*. 4974–4985.
- [12] Cong Fu, Chao Xiang, Changxu Wang, and Deng Cai. 2019. Fast approximate nearest neighbor search with the navigating spreading-out graph. *Proceedings of the VLDB Endowment* 12, 5 (2019), 461–474.
- [13] Chongming Gao, Shijun Li, Yuan Zhang, Jiawei Chen, Biao Li, Wenqiang Lei, Peng Jiang, and Xiangnan He. 2022. KuaiRand: An Unbiased Sequential Recommendation Dataset with Randomly Exposed Videos. In *Proceedings of the 31st ACM International Conference on Information & Knowledge Management*. 3953–3957.
- [14] Tiezheng Ge, Kaiming He, Qifa Ke, and Jian Sun. 2014. Optimized Product Quantization. *IEEE Transactions on Pattern Analysis and Machine Intelligence* 36, 4 (2014), 744–755.
- [15] Mihajlo Grbovic and Haibin Cheng. 2018. Real-time Personalization using Embeddings for Search Ranking at Airbnb. In *Proceedings of the 24th ACM SIGKDD International Conference on Knowledge Discovery & Data Mining*. 311–320.
- [16] Dandan Guo, Zhuo Li, He Zhao, Mingyuan Zhou, Hongyuan Zha, et al. 2022. Learning to re-weight examples with optimal transport for imbalanced classification. *Advances in Neural Information Processing Systems* 35 (2022), 25517–25530.
- [17] F. Maxwell Harper and Joseph A. Konstan. 2015. The MovieLens Datasets: History and Context. *ACM Transactions on Interactive Intelligent Systems (TiIS)* 5, 4 (2015).
- [18] Ruining He and Julian McAuley. 2016. Ups and Downs: Modeling the Visual Evolution of Fashion Trends with One-Class Collaborative Filtering. In *Proceedings of the 25th International Conference on World Wide Web*. 507–517.
- [19] Xiangnan He, Lizi Liao, Hanwang Zhang, Liqiang Nie, Xia Hu, and Tat-Seng Chua. 2017. Neural Collaborative Filtering. In *Proceedings of the 26th International Conference on World Wide Web*. 173–182.
- [20] Yun He, Xuxing Chen, Jiayi Xu, Renqin Cai, Yiling You, Jennifer Cao, Minhui Huang, Liu Yang, Yiqun Liu, Xiaoyi Liu, et al. 2024. MultiBalance: Multi-Objective Gradient Balancing in Industrial-Scale Multi-Task Recommendation System. *arXiv preprint arXiv:2411.11871* (2024).
- [21] Jonathan L. Herlocker, Joseph A. Konstan, and John Riedl. 2000. Explaining collaborative filtering recommendations. In *Proceedings of the 2000 ACM Conference on Computer Supported Cooperative Work*. 241–250.
- [22] Jun Hu and Ping Li. 2018. Collaborative Filtering via Additive Ordinal Regression. In *Proceedings of the Eleventh ACM International Conference on Web Search and Data Mining*. 243–251.
- [23] Jiahui Huang, Lan Zhang, Junhao Wang, Shanyang Jiang, Dongbo Huang, Cheng Ding, and Lan Xu. 2024. Utilizing Non-click Samples via Semi-supervised Learning for Conversion Rate Prediction. In *Proceedings of the 18th ACM Conference on Recommender Systems*. 350–359.
- [24] Jui-Ting Huang, Ashish Sharma, Shuying Sun, Li Xia, David Zhang, Philip Pronin, Janani Padmanabhan, Giuseppe Ottaviano, and Linjun Yang. 2020. Embedding-based Retrieval in Facebook Search. In *Proceedings of the 26th ACM SIGKDD International Conference on Knowledge Discovery & Data Mining*. 2553–2561.
- [25] Po-Sen Huang, Xiaodong He, Jianfeng Gao, Li Deng, Alex Acero, and Larry Heck. 2013. Learning deep structured semantic models for web search using

- clickthrough data. In *Proceedings of the 22nd ACM International Conference on Information & Knowledge Management*. 2333–2338.
- [26] Herve Jegou, Matthijs Douze, and Cordelia Schmid. 2011. Product Quantization for Nearest Neighbor Search. *IEEE Transactions on Pattern Analysis and Machine Intelligence* 33, 1 (2011), 117–128.
- [27] Yehuda Koren, Robert Bell, and Chris Volinsky. 2009. Matrix Factorization Techniques for Recommender Systems. *Computer* 42, 8 (2009), 30–37.
- [28] Yehuda Koren and Joe Sill. 2011. OrdRec: an ordinal model for predicting personalized item rating distributions. In *Proceedings of the Fifth ACM Conference on Recommender Systems*. 117–124.
- [29] Ping Li, Christopher J. C. Burges, and Qiang Wu. 2007. McRank: learning to rank using multiple classification and gradient boosting. In *Proceedings of the 21st International Conference on Neural Information Processing Systems*. 897–904.
- [30] Pengcheng Li, Runze Li, Qing Da, An-Xiang Zeng, and Lijun Zhang. 2020. Improving Multi-Scenario Learning to Rank in E-commerce by Exploiting Task Relationships in the Label Space. In *Proceedings of the 29th ACM International Conference on Information & Knowledge Management*. 2605–2612.
- [31] Tsung-Yi Lin, Priya Goyal, Ross Girshick, Kaiming He, and Piotr Dollár. 2017. Focal Loss for Dense Object Detection. In *2017 IEEE International Conference on Computer Vision (ICCV)*. 2999–3007.
- [32] Yuqi Liu, Bin Cao, and Jing Fan. 2022. Improving the accuracy of learning example weights for imbalance classification. In *International Conference on Learning Representations*.
- [33] Jiaqi Ma, Zhe Zhao, Xinyang Yi, Jilin Chen, Lichan Hong, and Ed H. Chi. 2018. Modeling Task Relationships in Multi-task Learning with Multi-gate Mixture-of-Experts. In *Proceedings of the 24th ACM SIGKDD International Conference on Knowledge Discovery & Data Mining*. 1930–1939.
- [34] Xiao Ma, Liqin Zhao, Guan Huang, Zhi Wang, Zelin Hu, Xiaoqiang Zhu, and Kun Gai. 2018. Entire Space Multi-Task Model: An Effective Approach for Estimating Post-Click Conversion Rate. In *The 41st International ACM SIGIR Conference on Research & Development in Information Retrieval*. 1137–1140.
- [35] Yu A. Malkov and D. A. Yashunin. 2020. Efficient and Robust Approximate Nearest Neighbor Search Using Hierarchical Navigable Small World Graphs. *IEEE Transactions on Pattern Analysis and Machine Intelligence* 42, 4 (2020), 824–836.
- [36] Mark Mathieson. 1996. Ordinal models for neural networks. *Neural Networks in Financial Engineering* (1996).
- [37] Peter McCullagh. 1980. Regression models for ordinal data. *Journal of the Royal Statistical Society: Series B (Methodological)* 42, 2 (1980), 109–127.
- [38] Denis Parra, Alexandros Karatzoglou, Xavier Amatriain, Idil Yavuz, et al. 2011. Implicit feedback recommendation via implicit-to-explicit ordinal logistic regression mapping. *Proceedings of the CARS-2011* 5 (2011).
- [39] Bercedis Peterson and Frank E Harrell Jr. 1990. Partial Proportional Odds Model for Ordinal Response Variables. *Journal of the Royal Statistical Society: Series C (Applied Statistics)* 39, 2 (1990), 205–217.
- [40] Marco Tulio Ribeiro, Nivio Ziviani, Edleno Silva De Moura, Itamar Hata, Anisio Lacerda, and Adriano Veloso. 2015. Multiobjective Pareto-Efficient Approaches for Recommender Systems. *ACM Transactions on Intelligent Systems and Technology (TIST)* 5, 4 (2015).
- [41] Mario Rodriguez, Christian Posse, and Ethan Zhang. 2012. Multiple objective optimization in recommender systems. In *Proceedings of the Sixth ACM Conference on Recommender Systems*. 11–18.
- [42] Badrul Sarwar, George Karypis, Joseph Konstan, and John Riedl. 2001. Item-based collaborative filtering recommendation algorithms. In *Proceedings of the 10th International Conference on World Wide Web*. 285–295.
- [43] Xiang-Rong Sheng, Jingyue Gao, Yueyao Cheng, Siran Yang, Shuguang Han, Hongbo Deng, Yuning Jiang, Jian Xu, and Bo Zheng. 2023. Joint Optimization of Ranking and Calibration with Contextualized Hybrid Model. In *Proceedings of the 29th ACM SIGKDD Conference on Knowledge Discovery and Data Mining*. 4813–4822.
- [44] Derun Song, Enneng Yang, Guibing Guo, Li Shen, Linying Jiang, and Xingwei Wang. 2024. Multi-Scenario and Multi-Task Aware Feature Interaction for Recommendation System. *ACM Transactions on Knowledge Discovery from Data* (2024).
- [45] Xiaoyuan Su and Taghi M. Khoshgoftaar. 2009. A survey of collaborative filtering techniques. *Advances in Artificial Intelligence* 2009 (2009).
- [46] Hongyan Tang, Junning Liu, Ming Zhao, and Xudong Gong. 2020. Progressive Layered Extraction (PLE): A Novel Multi-Task Learning (MTL) Model for Personalized Recommendations. In *Proceedings of the 14th ACM Conference on Recommender Systems*. 269–278.
- [47] Xuewen Tao, Mingming Ha, Qiongxiu Ma, Hongwei Cheng, Wenfang Lin, Xiaobo Guo, Linxun Cheng, and Bing Han. 2023. Task Aware Feature Extraction Framework for Sequential Dependence Multi-Task Learning. In *Proceedings of the 17th ACM Conference on Recommender Systems*. 151–160.
- [48] Gerhard Tutz. 2022. Ordinal regression: A review and a taxonomy of models. *Wiley Interdisciplinary Reviews: Computational Statistics* 14, 2 (2022).
- [49] Chao Wang, Hengshu Zhu, Chen Zhu, Chuan Qin, Enhong Chen, and Hui Xiong. 2023. SetRank: A Setwise Bayesian Approach for Collaborative Ranking in Recommender System. *ACM Transactions on Information Systems* 42, 2 (2023), 1–32.
- [50] Hao Wang, Tai-Wei Chang, Tianqiao Liu, Jianmin Huang, Zhichao Chen, Chao Yu, Ruopeng Li, and Wei Chu. 2022. ESCM2: Entire Space Counterfactual Multi-Task Model for Post-Click Conversion Rate Estimation. In *Proceedings of the 45th International ACM SIGIR Conference on Research and Development in Information Retrieval*. 363–372.
- [51] Hongwei Wang, Miao Zhao, Xing Xie, Wenjie Li, and Minyi Guo. 2019. Knowledge Graph Convolutional Networks for Recommender Systems. In *The World Wide Web Conference*. 3307–3313.
- [52] Richard Williams. 2006. Generalized ordered logit/partial proportional odds models for ordinal dependent variables. *The stata journal* 6, 1 (2006), 58–82.
- [53] Dongbo Xi, Zhen Chen, Peng Yan, Yinger Zhang, Yongchun Zhu, Fuzhen Zhuang, and Yu Chen. 2021. Modeling the Sequential Dependence among Audience Multi-step Conversions with Multi-task Learning in Targeted Display Advertising. In *Proceedings of the 27th ACM SIGKDD Conference on Knowledge Discovery & Data Mining*. 3745–3755.
- [54] Fen Xia, Tie-Yan Liu, Jue Wang, Wensheng Zhang, and Hang Li. 2008. Listwise approach to learning to rank: theory and algorithm. In *Proceedings of the 25th International Conference on Machine Learning*. 1192–1199.
- [55] Xinyang Yi, Ji Yang, Lichan Hong, Derek Zhiyuan Cheng, Lukasz Heldt, Aditee Kumthekar, Zhe Zhao, Li Wei, and Ed Chi. 2019. Sampling-bias-corrected neural modeling for large corpus item recommendations. In *Proceedings of the 13th ACM Conference on Recommender Systems*. 269–277.
- [56] Tianhe Yu, Saurabh Kumar, Abhishek Gupta, Sergey Levine, Karol Hausman, and Chelsea Finn. 2020. Gradient surgery for multi-task learning. In *Proceedings of the 34th International Conference on Neural Information Processing Systems*. 5824–5836.
- [57] Yantao Yu, Weipeng Wang, Zhoutian Feng, and Daiyue Xue. 2021. A dual augmented two-tower model for online large-scale recommendation. In *DLP-KDD*.
- [58] Fuzheng Zhang, Nicholas Jing Yuan, Defu Lian, Xing Xie, and Wei-Ying Ma. 2016. Collaborative Knowledge Base Embedding for Recommender Systems. In *Proceedings of the 22nd ACM SIGKDD International Conference on Knowledge Discovery and Data Mining*. 353–362.
- [59] Han Zhang, Yunjing Jiang, Mingming Li, Haowei Yuan, and Wen-Yun Yang. 2024. pEBR: A Probabilistic Approach to Embedding Based Retrieval. *arXiv preprint arXiv:2410.19349* (2024).
- [60] Qihua Zhang, Junning Liu, Yuzhuo Dai, Yiyan Qi, Yifan Yuan, Kunlun Zheng, Fan Huang, and Xianfeng Tan. 2022. Multi-Task Fusion via Reinforcement Learning for Long-Term User Satisfaction in Recommender Systems. In *Proceedings of the 28th ACM SIGKDD Conference on Knowledge Discovery and Data Mining*. 4510–4520.
- [61] Guorui Zhou, Xiaoqiang Zhu, Chenru Song, Ying Fan, Han Zhu, Xiao Ma, Yanghui Yan, Junqi Jin, Han Li, and Kun Gai. 2018. Deep Interest Network for Click-Through Rate Prediction. In *Proceedings of the 24th ACM SIGKDD International Conference on Knowledge Discovery & Data Mining*. 1059–1068.
- [62] Feng Zhu, Mingjie Zhong, Xinxing Yang, Longfei Li, Lu Yu, Tiehua Zhang, Jun Zhou, Chaochao Chen, Fei Wu, Guanfeng Liu, and Yan Wang. 2023. DCMT: A Direct Entire-Space Causal Multi-Task Framework for Post-Click Conversion Estimation. In *Proceedings of the 39th International Conference on Data Engineering*. 3113–3125.

A APPENDIX

A.1 Embedding Based Collaborative Filtering

Embedding-based collaborative filtering (ECF) is widely deployed in modern recommender systems. Due to the limited expressiveness of linear models, deep learning techniques are widely employed [19]. In large-scale, cascade-based pipelines [7], ECF often pairs with nearest neighbor search [35] to produce a relatively small, personalized candidate set for downstream ranking. As illustrated in Figure 6, the workflow typically involves offline and online stages.

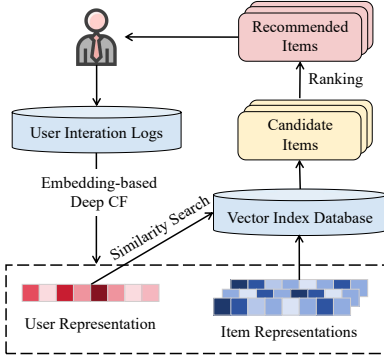


Figure 6: An illustration of real-world recommender system design when applying deep-learning based collaborative filtering to generate relevant candidate items.

Offline Stage: A trained ECF model generates user and item embeddings separately. The item embeddings are then indexed for approximate nearest neighbor search.

Online Stage: User embeddings are computed on the fly to capture instant preferences, and nearest neighbor search retrieves relevant items from the indexed embedding database. Because of strict latency constraints, the candidate set must be truncated before fine-grained ranking.

This coarse-grained candidate generation imposes two key requirements. **(1) Independent Embeddings:** User and item embeddings must be generated independently, precluding user-item cross interaction features to avoid train-inference mismatch. **(2) Euclidean (or Isomorphic) Metric Space:** Indexing methods typically rely on Euclidean distance [8, 10, 12, 14, 26, 35]. Cosine similarity is isomorphic to Euclidean distance because vectors are ℓ_2 -normalized, ensuring higher cosine similarity corresponds to a smaller Euclidean distance.

Prior paradigm (feedback-wise) ECF uses multiple feedback to model user preference. Each feedback type would require its own index, increasing system complexity and leading to suboptimal performance due to separate retrieval and truncation. In addition, a fusion heuristic is needed to merge the results from the multiple independent retrieval process. A typical fusion strategy is a multiplicative formula. For example,

$$Score_{final} = Score_{task_1}^\alpha \cdot Score_{task_2}^\beta \cdot Score_{task_3}^\gamma$$

Such formula may not fully capture the complex relationship between feedback and suffers from precision issues and inefficient parameter searching as the number of tasks grows. This underscores the importance of our proposed approach.

Table 8: Statistics of all datasets. The number of users and items in the AE series datasets is not disclosed. #Pos₁ and #Pos₂ denotes the counts for click and pay in e-commercial datasets, likes and follows for video datasets.

Dataset	#User	#Item	Split	Total	#Pos ₁	#Pos ₂
Ali-CCP	0.24M	0.47M	train	41.9M	1.63M	8.4K
			test	27.2M	0.99M	4.7K
AE-ES	/	/	train	22.3M	0.57M	12.9K
			test	9.3M	0.27M	6.2K
AE-FR	/	/	train	18.2M	0.34M	9.1K
			test	8.8M	0.20M	5.4K
AE-NL	/	/	train	1.8M	0.035M	1.2K
			test	5.6M	0.14M	4.9K
AE-US	/	/	train	20M	0.29M	7.0K
			test	7.5M	0.16M	3.9K
KR-Pure	24.9K	6.8K	train	0.72M	15.8K	0.86K
			test	0.2M	4K	0.28K
KR-1K	1K	2.4M	train	4.9M	94K	5.7K
			test	1.8M	35K	2.3K
ML-1M	6K	3.7K	train	0.7M	0.17M	/
			test	0.3M	0.058M	/
ML-20M	138K	27K	train	13.9M	3.2M	/
			test	6.1M	1.3M	/
RetailR	1.4M	0.24M	train	2.13M	56K	9.8K
			test	0.63M	36K	12.7K

Table 9: Number of features used in each dataset.

Feature Type	AliCCP	AE	ML-1M	ML-20M	KR	RetailR
User Feature	9	33	4	1	30	1
Item Feature	5	47	2	2	63	1

A.2 Reproducibility

A.2.1 Dataset Preprocess. To comply with the independent embedding requirement, we omit cross features. Specifically, the AliCCP dataset includes 4 cross features, named as 508, 509, 702, 853, which are not used in our experiments. For the rest datasets, there is no such features, thus we use all the features. To maintain consistent learning speed among features and mitigate outlier effects, numerical features are discretized into 50 bins using percentile-based bucketization on the training set. The same bin boundaries are then applied to the test set. Table 9 summarizes the quantity of used features for each dataset.

For the AE series datasets, which originate from a personalized e-commerce search scenario (user search merchandises with a query), each user-query pair is treated as a distinct user to align with the modeling on other datasets.

If official splits are provided, we adopt them directly. Otherwise (e.g., MovieLens), we perform the chronological split from Section 4.1.1. A 10% subset of the training data serves as the validation set for hyperparameter tuning. A detailed version of the datasets are given in Table 8.

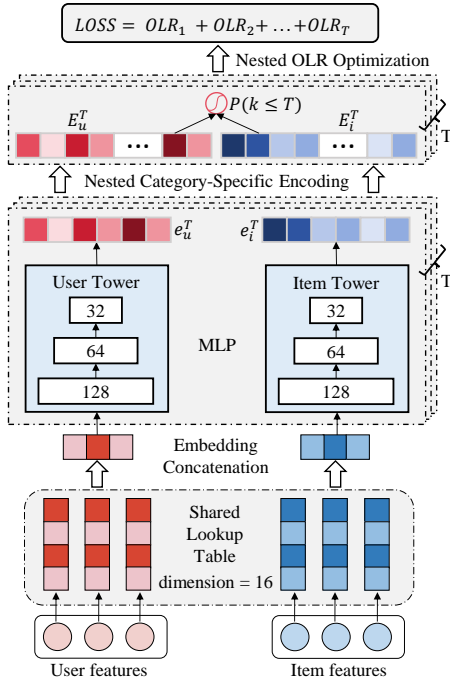


Figure 7: The implementation details of the GNOLR, where the twin tower architecture is consistent across all methods.

A.2.2 Hyperparameters. We use a batch size of 1024 for pointwise single-task and multi-task training to ensure at least one positive sample per feedback in each batch. For listwise and retrieval experiments, where the model compares positive and negative samples from the same user, we restructure each user’s interaction history into lists, preserving intra-user interactions. To prevent excessively long sequences, user interaction lists exceeding 500 items are randomly split into smaller sublists. We then adopt a batch size of 32 lists, enabling effective listwise and pairwise comparisons within each batch.

All methods employ the Adam optimizer, with hyperparameters determined via grid search for each dataset and method over 200 epoch runs. For all methods, the optimal learning rate is 0.05 (ML-1M), 0.5 (ML-20M), 0.01 (AliCCP), 0.05 (KuaiRand), 5 (AE) and 0.05 (RetailRocket).

For all methods, we adopt a Twin Tower base architecture with an embedding dimension of 16 and an MLP structure of $\{128, 64, 32\}$, as illustrated in Figure 7. The embedding lookup tables for each feature are randomly initialized and shared across tasks. We use LeakyReLU activations and no dropout. Our experiments show that these methods exhibit low sensitivity to variations in the network backbone. Thus we use the same backbone for all methods and all datasets, except that we use $\{256, 128, 64\}$ MLP for naive Neural OLR on multi-task (two tasks) setting to ensure the fairness in parameter quantity. **The code** is provided in <https://github.com/FuCongResearchSquad/GNOLR>

For GNOLR, additional hyperparameters must be specified: $\{a_c\}$ and γ . We directly set $\{a_c\}$ according to the calculation in Section 3.4 and perform a grid search to find the optimal γ . Table 10 summarizes these configurations.

Table 10: Optimal a_c (Section 3.4) and γ (grid-search) of GNOLR used in different datasets and tasks. The listwise and retrieval tasks use the same configuration as the single-task.

Dataset	Single-Task		Multi-Task		
	a_1	γ	a_1	a_2	γ
AliCCP	3.2343	7.00	3.2343	8.5681	4.0
AE-ES	3.6003	7.00	3.6003	7.4130	1.0
AE-FR	3.8880	7.00	3.8880	7.5351	3.0
AE-US	4.0931	8.00	4.0931	7.8353	2.0
AE-NL	3.7294	2.80	3.7294	7.0835	3.0
KR-Pure	3.8181	7.30	3.8181	6.6975	2.8
KR-1K	3.9332	2.80	3.9332	6.7388	2.5
ML-1M	1.2295	2.57	/	/	/
ML-20M	1.2560	3.00	/	/	/
RetailR	3.3682	2.00	3.3682	4.8018	2.0

Table 11: The AUC performance comparison of various listwise ranking methods across multiple datasets. The best results (statistically significant) are highlighted in bold, while the second-best are underlined. λ Rank is LambdaRank.

Dataset	RankNet	λ Rank	ListNet	S2SRank	SetRank	JRC	GNOLR _L
AliCCP	<u>0.5696</u>	0.5681	0.5577	0.5658	0.5682	0.5009	0.6232
AE-ES	<u>0.7332</u>	0.7297	0.6403	0.7293	0.7200	0.6323	0.7388
AE-FR	<u>0.7330</u>	0.7277	0.7298	0.7294	0.7216	0.6428	0.7385
AE-US	<u>0.7046</u>	0.6996	0.6924	0.7009	0.6874	0.6256	0.7061
AE-NL	<u>0.6923</u>	0.6897	0.6583	0.6915	0.6831	0.6419	0.7301
KR-Pure	0.6396	0.6345	0.6355	0.6408	0.6384	<u>0.7835</u>	0.8326
KR-1K	0.6321	0.5611	0.6531	0.7047	0.5354	<u>0.7964</u>	0.8834
ML-1M	0.7477	0.7327	0.7305	0.7443	0.7409	<u>0.7937</u>	0.8080
ML-20M	0.7138	0.7007	0.7101	0.7187	0.7154	<u>0.7801</u>	0.8072
RetailR	0.6292	0.6238	0.5592	0.6256	0.6136	<u>0.7275</u>	0.7294

A.2.3 Training Stability. Because $P(k = c|\mathbf{x}) = P(k \leq c|\mathbf{x}) - P(k \leq c - 1|\mathbf{x})$, the negative log-likelihood requires that this difference remain positive. To prevent numerical instability, we clip these probabilities to $(1e^{-6}, \infty)$.

A.3 Additional Experimental Results

A.3.1 Listwise GNOLR. GNOLR is inherently a pointwise ranking and retrieval method, which does not explicitly enforce user-specific dependencies. However, it can be combined with a listwise loss to enhance personalization, as demonstrated in our experiments. Specifically, in the OLR framework, $\gamma\mathcal{K}(E_u^c, E_i^c)$ serves as the model’s logit. To incorporate listwise learning, we reuse this logit in a ListNet-style loss:

$$Loss_{ListNet} = - \sum_{l=1}^L \sum_{x^+ \in \mathcal{P}} \frac{e^{\gamma\mathcal{K}(E_u^+, E_i^+)}}{\sum_{x \in \mathcal{P} \cup \mathcal{N}} e^{\gamma\mathcal{K}(E_u, E_i)}}, \quad (8)$$

where L is the number of lists, \mathcal{P} denotes the set of positive samples within one list, and \mathcal{N} denotes the set of negative samples within one list. The final loss function combines the GNOLR loss and the listwise loss:

$$Loss = Loss_{GNOLR} + Loss_{ListNet} \quad (9)$$

Table 12: The positive sample weight for each task and dataset, where the negative sample weight is fixed as 1. For example, we set weight=10 for positive clicked samples and weight=100 for positive purchased samples. BCE and JRC are only evaluated under the single-task setting.

Dataset	AliCCP	AE	KR-Pure	KR-1K	ML	RetailR
BCE	[10]	[10]	[10]	[10]	[2]	[10]
JRC	[10]	[10]	[10]	[10]	[2]	[10]
NSB	[10,100]	[100,10]	[100,1]	[50,100]	/	[10,100]
ESMM	[10,50]	[10,50]	[100,10]	[100,50]	/	[10,50]
ESCM ² -IPS	[10,50]	[15,50]	[100,1]	[50,100]	/	[10,50]
ESCM ² -DR	[10,50]	[50,100]	[100,1]	[50,100]	/	[10,50]
DCMT	[10,50]	[10,50]	[100,1]	[50,100]	/	[10,50]
NISE	[10,50]	[10,50]	[50,1]	[50,100]	/	[5,50]
TAFE	[10,50]	[10,50]	[50,20]	[50,100]	/	[10,50]

Table 13: Performance comparison with multiple implicit feedback types on KR-1K. Single refers to single task prediction for each feedback as baseline.

	Click	Like	Follow	Forward
Single	<u>0.7061</u>	<u>0.8934</u>	<u>0.7532</u>	<u>0.7495</u>
NSB	0.7024	0.8885	0.7197	0.5991
ESMM	0.6839	0.8916	0.7354	0.5967
TAFE	0.6540	0.8576	0.7326	0.7339
GNOLR	0.7097	0.9101	0.9023	0.7947

Table 14: Performance comparison between Manual $\{a_c\}$ and learned on KR-1K.

$(auc/\{a_c\})$	Manual	Learned	Learned w/ target
Like	0.9120 /3.9	0.9098/3.0	0.9114/2.6
Follow	0.8204 /6.7	0.7233/3.7	0.7566/6.3

A.3.2 Listwise AUC. Table 11 shows the AUC results for the listwise experiment, complementing the GAUC results in Table 3. Pairwise, setwise, and listwise baselines struggle to balance AUC (calibration) and GAUC (personalization). By contrast, GNOLR_L increases GAUC without degrading AUC, demonstrating a more effective balance.

A.3.3 Re-weighting in Multi-Task. Table 16 reports the multi-task AUC without sample re-weighting, complementing the single-task results in Table 2 and 4. While sample re-weighting improves cross-entropy-based baselines’ performance on imbalanced data, it introduces two main drawbacks.

(1) The optimal positive weights vary widely by dataset and task (presented in Table 12), making Pareto optimization difficult—especially as tasks grow and user distributions evolve in real-world scenarios. GNOLR avoids these complications, achieving its best performance without re-weighting.

(2) Re-weighting does not resolve the disjoint embedding space inherent in task-independent modeling. Figure 8 (complementing Figure 4) visualizes all item embeddings’ directions when all user embeddings are fixed to an upward vector.

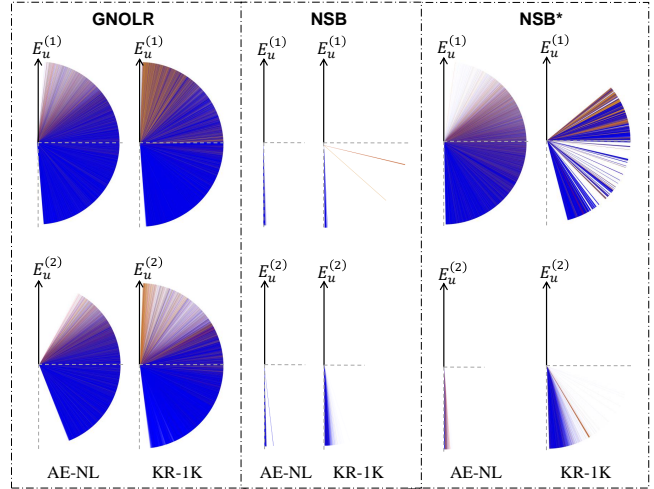


Figure 8: Visualization of the angular distribution between user and item embeddings on KR-1K and AE-NL datasets for different methods. $E_u^{(1)}$ is the sub-embedding of GNOLR, and $E_u^{(2)}$ is the unified embedding of GNOLR. For NSB and NSB*, $E_u^{(1)}$ is the embedding of the denser task, and $E_u^{(2)}$ is the embedding of the sparse task. NSB* is the sample re-weighted version of NSB.

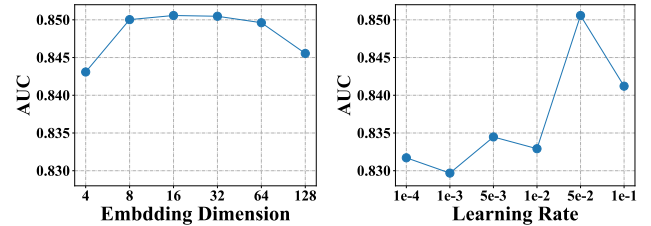


Figure 9: Parameter sensitivity experiment results on KR-Pure. From left to right: Embedding Dimension, Learning Rate.

Without re-weighting, baselines often push item embeddings near 180° from the user vector—unusable for nearest neighbor search. Even with optimal re-weighting, dense tasks (e.g., CTR) spread items more favorably ($< 45^\circ$ from the user), while items in sparse tasks (e.g., conversion) still cluster near 180° . Especially, on the KR-1K dataset, multiple disjoint clusters emerge. In contrast, GNOLR produces a continuous and smooth sector shape, placing positive items closer and negative items farther, thus offering a superior unified embedding space.

Notably, GNOLR’s sub-embeddings also establish favorable spatial proximity between users and items, reflecting strong alignment with user engagement. The shrinkage of unified embedding distribution compared with the sub-embedding may be due to the impact of reshaping factor γ .

A.3.4 Additional Parameter Sensitivity Experiments. Figure 9 shows that GNOLR’s performance remains relatively stable with varying

Table 15: Performance comparison with different backbone architectures on KR-1K.

Backbone	Task	NSB	ESMM	ESCM-IPS	ESCM-DR	DCMT	NISE	TAFE	Neural OLR	GNOLR
MMoE	Like	0.8867	0.8861	0.8960	0.8975	0.9017	0.8885	0.8915	<u>0.9105</u>	0.9115
	Follow	0.7176	0.7164	<u>0.7952</u>	0.7783	0.7837	0.6799	0.7204	0.6966	0.8188
MMFI	Like	0.8969	0.8994	0.8988	0.8861	0.8935	0.9020	0.9048	<u>0.9108</u>	0.9127
	Follow	0.7432	0.7081	<u>0.7950</u>	0.7932	0.7933	0.6870	0.7545	0.6930	0.8141

Table 16: Multi-Task Ranking Results (AUC) w/o Pos Sample Weights.

Task	Dataset	NSB	ESMM	ESCM ² -IPS	ESCM ² -DR	DCMT	NISE	TAFE	GNOLR
CTR	AliCCP	0.4994	0.4999	0.4992	0.5004	0.5771	<u>0.5919</u>	0.5810	0.6153
	AE-ES	0.5000	0.4999	0.4999	0.4998	0.5001	0.5003	<u>0.5004</u>	0.7372
	AE-FR	0.5006	0.5061	0.5046	0.4998	<u>0.5132</u>	0.5006	0.5003	0.7370
	AE-US	0.5003	0.5007	0.5025	0.5008	<u>0.5092</u>	0.4993	0.5010	0.6971
	AE-NL	0.5222	0.4983	0.5397	0.4778	0.5216	<u>0.5628</u>	0.5378	0.7277
CTCVR	AliCCP	0.5015	0.5004	0.5003	0.5028	<u>0.5637</u>	0.5050	0.5308	0.5997
	AE-ES	0.5034	0.5037	0.5106	<u>0.7036</u>	0.5074	0.5030	0.5007	0.8827
	AE-FR	<u>0.6133</u>	0.5353	0.5122	0.5351	0.5114	0.5194	0.5425	0.8793
	AE-US	0.5022	<u>0.6012</u>	0.5307	0.5034	0.5522	0.5063	0.5044	0.8663
Like	AE-NL	0.5195	<u>0.5216</u>	0.5546	<u>0.7022</u>	0.5712	0.6337	0.5900	0.8343
	KR-Pure	0.5099	0.4989	<u>0.5224</u>	<u>0.4977</u>	0.4937	0.4990	0.4985	0.8456
Follow	KR-1K	0.5689	<u>0.6806</u>	0.5720	0.5125	0.5555	0.5540	0.6720	0.9087
	KR-Pure	0.5334	0.5435	0.5384	0.5365	<u>0.5447</u>	0.5378	0.5315	0.7161
Follow	KR-1K	0.5981	0.6209	0.5996	0.5806	0.5844	0.5937	<u>0.6260</u>	0.8165

embedding sizes, while an optimal learning rate exists for GNOLR, which is the same for other baselines.

A.3.5 Experiments with Alternative Backbone Architectures. To further validate the architectural flexibility of GNOLR, we conduct additional experiments replacing the original backbone (Twin Tower encoders with standard MLPs) with two alternative architectures: MMoE [33] and MMFI [44]. All compared methods (including baselines) are re-implemented with these backbones under identical training protocols. As summarized in Table 15, GNOLR consistently outperforms baselines across all backbone architectures, with all methods showing improved performance from advanced structures.

A.3.6 Extension to Multiple Feedback Types. While most baselines in the main experiments only model two types of implicit feedback, we further evaluate GNOLR’s scalability with **four implicit feedback types** on the KR-1K dataset. We select adaptably designed

baselines (NSB, ESMM, TAFE) and modify their implementations for multi-feedback processing. As shown in Table 13, GNOLR demonstrates a strong ability to model long-range and progressive implicit user preferences.

A.3.7 Learning vs. Manual Selection for Ordinal Thresholds $\{a_c\}$. As mentioned in Section 3.4, the thresholds $\{a_c\}$ can be learned jointly with the model. To validate whether our manually selected $\{a_c\}$ is reasonable, we implemented two parameter learning schemes for comparison with the manual selection approach: (1) simply preserving the inherent order constraint of $\{a_c\}$, and (2) additionally imposing a regularization penalty to push the learned $\{a_c\}$ closer to the manual value. The result are shown in Table 14, where we observe that the model can hardly learn optimal $\{a_c\}$ for sparse targets.